Quantum spatial correlations in the optical parametric oscillator with spherical mirrors

L. A. Lugiato and I. Marzoli
Dipartimento di Fisica, Istituto Nazionale di Fisica della Materia, Università degli Studi di Milano, Via Celoria 16, I-20133 Milano, Italy
(Received 26 June 1995)

We consider a quantum model for a degenerate optical parametric oscillator below threshold in a cavity with spherical mirrors. The spatial correlation function of a generic quadrature component of the signal field is calculated analytically in terms of an expansion over the Gauss-Laguerre modes. The critical behavior and the quantum image phenomenon, which emerge when threshold is approached, are described in detail. We calculate also the spatial correlation function of the intensity fluctuations, which can be more easily measured by direct detection and exhibits the same qualitative features.

PACS number(s): 42.50.Dv, 42.65.−k, 42.50.Ne

I. INTRODUCTION

It is well known that the radiation field, interacting with nonlinear media, can give rise to phenomena of spontaneous spatial pattern formation in the planes orthogonal to the direction of propagation [1]. A distinguished feature of optics, with respect to other disciplines (e.g., hydrodynamics or nonlinear chemical reactions) that are more traditional in the study of pattern formation, is the presence of noteworthy quantum aspects [2–5]. The analysis of the quantum effects is also related to the description of the spatial aspects of nonclassical (squeezed) states of the radiation field [5–9]. In particular, the analysis of [5] focused on the spatial correlation function of a generic quadrature component of the electric field, showing in general its useful connection with the measurement of the spectrum of squeezing. Considering the especially simple model of the optical parametric oscillator (OPO) below threshold, the spatial correlation function of the quantum-noise-generated signal field has been calculated analytically in Ref. [5] for the case of cavity with plane mirrors. It has been shown that, approaching threshold, one finds a critical behavior with divergence of the correlation length, which provides a necessary completion of the classic analogy with second-order phase transitions in equilibrium systems [10,11]. Furthermore, the analysis of [5] showed that, under appropriate conditions, the correlation function exhibits a spatial modulation identical to that which characterizes the stripe (roll) pattern that appears above threshold [12]. The interest of this phenomenon lies in the fact that below threshold the signal field has a spatial intensity distribution that is uniform on average; hence this field configuration corresponds to an "image" that exhibits a spatial structure only in the correlation function. For this phenomenon we use the name "quantum image"; an extensive discussion of this concept can be found in [4]. The purpose of this paper is twofold and both aspects described below are intended to produce a theory that can provide a realistic guideline for a future experimental observation of these effects.

First, because the model of cavity with plane mirrors is idealized, we consider here the standard case of a cavity with spherical mirrors and calculate analytically the spatial correlation function of the signal field emitted by the OPO below threshold. Second, we consider here not only the correlation function of a generic quadrature component but also evaluate the spatial correlation function of the intensity, which can be easily measured by direct detection, avoiding the use of a local oscillator.

In Sec. II we recall the definition of the spatial correlation function of the quadrature phase operators and its connection with the spectrum of squeezing. Section III introduces the quantum model that describes a degenerate optical parametric oscillator below threshold with spherical mirrors. The equal time spatial correlation function of a generic quadrature component is calculated in Sec. IV and some numerical examples are discussed in Sec. V. The same correlation function is analyzed in the frequency domain in Sec. VI. Section VII contains the calculation and the discussion of the equal time spatial intensity correlation function, while in Sec. VIII the same correlation function is analyzed in the frequency domain. Finally, Sec. IX contains conclusions.

II. SPATIAL CORRELATION FUNCTION OF QUADRATURE PHASE OPERATORS

In this section we briefly review the notions of balanced homodyne detection [8,13], spectrum of squeezing, and spatial correlation function [5,8]. These topics and the connection between the spectrum of squeezing and the space-time correlation function have been covered in [5]; even though in [5] the analysis was limited to the special case of plane waves, the main results can be generalized to different orthonormal sets, e.g., Gauss-Laguerre modes. On the basis of the expression of the spectrum of squeezing given in [8], we calculate the relevant spatial correlation function, which describes the degree of spatial order in the field generated by quantum noise.

The signal field $A_{\text{out}}(\mathbf{x},t)$ at the output of the OPO and the local oscillator field (LOF), which lies in a classical stationary coherent state $\alpha_L(\mathbf{x})$, are combined by a beam splitter, with reflection and transmission coefficients $r=t=1/\sqrt{2}$ (Fig. 1). The vector $\mathbf{x}=(x,y)$ lies in a plane perpendicular to the direction of propagation of the beam. The fields emerging from the beam splitter are

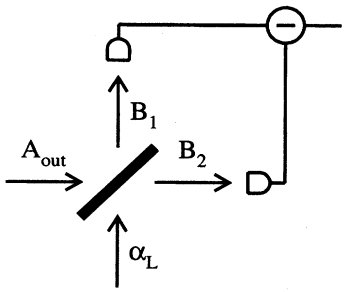

FIG. 1. Balanced homodyne detection scheme.

$$B_1(\mathbf{x},t)=\frac{1}{\sqrt{2}}[A_{\rm out}(\mathbf{x},t)+\alpha_L(\mathbf{x})], \tag{1}$$

$$B_2(\mathbf{x},t)=\frac{1}{\sqrt{2}}[A_{\rm out}(\mathbf{x},t)-\alpha_L(\mathbf{x})]; \tag{2}$$

their intensities are measured by two photodetectors and then subtracted in such a way that the homodyne signal is proportional to the quadrature operator [5,8,13]:

$$E_H^{\rm out}(t)=\frac{1}{N^{1/2}}\int d^2\mathbf{x}[\alpha_L(\mathbf{x})A_{\rm out}^{\dagger}(\mathbf{x},t)+\alpha_L^*(\mathbf{x})A_{\rm out}(\mathbf{x},t)] \ , \tag{3}$$

$$N=\int d^2\mathbf{x}|\alpha_L(\mathbf{x})|^2 \ . \tag{4}$$

The fluctuations around a stationary state are described by the spectrum

$$V(\omega)=\int_{-\infty}^{+\infty}dt\ e^{-i\omega t}\langle\delta E_H^{\rm out}(t)\,\delta E_H^{\rm out}(0)\rangle \ , \tag{5}$$

where

$$\delta E_H^{\rm out}(t)=E_H^{\rm out}(t)-\langle E_H^{\rm out}\rangle \tag{6}$$

and $\langle E_H^{\rm out}\rangle$ is the stationary mean value. By inserting Eqs. (3) and (4) into Eq. (5) and taking into account the commutation rule $[A_{\rm out}(\mathbf{x},t),A_{\rm out}^{\dagger}(\mathbf{x}',t')]=\delta(\mathbf{x}-\mathbf{x}')\delta(t-t')$, one obtains

$$V(\omega)=1+S(\omega) \ , \tag{7}$$

with

$$S(\omega)=\int_{-\infty}^{+\infty}dt\ e^{-i\omega t}\langle:\delta E_H^{\rm out}(t)\,\delta E_H^{\rm out}(0):\rangle \ , \tag{8}$$

where : : means normal and time ordering. The constant part of Eq. (7) represents the shot-noise level, while the second term $S(\omega)$ is responsible for possible excess noise and nonclassical effects: in particular, for $S(\omega)=-1$ one has complete suppression of quantum noise at the corresponding frequency ω in the observable $E_H^{\rm out}(t)$. In the following we will consider a single-ended cavity containing a nonlinear medium; the coupling mirror has the reflection coefficient $r_c\approx 1$ and the transmission coefficient $t_c=(1-r_c^2)^{1/2}$. According to the input-output formulation [14] it is possible to express the outgoing field $A_{\rm out}(\mathbf{x},t)$ in terms of the intracavity field $A(\mathbf{x},t)$ and of the incident field $A_{\rm in}(\mathbf{x},t)$ as

$$A_{\rm out}(\mathbf{x},t)=\sqrt{2\gamma}A(\mathbf{x},t)-A_{\rm in}(\mathbf{x},t) \ , \tag{9}$$

where $\gamma=ct_c^2/2\mathscr{L}$ is the cavity linewidth, with $\mathscr{L}$ being the cavity round-trip length. It can be proved [15] that when the input field is in a coherent state the spectrum of $A_{\rm out}(\mathbf{x},t)$ is proportional to that of the intracavity field since the contribution of $A_{\rm in}(\mathbf{x},t)$ vanishes:

$$S(\omega)=2\gamma\int_{-\infty}^{+\infty}dt\ e^{-i\omega t}\langle:\delta E_H(t)\,\delta E_H(0):\rangle \ , \tag{10}$$

where

$$E_H(t)=\frac{1}{N^{1/2}}\int d^2\mathbf{x}[\alpha_L(\mathbf{x})A^{\dagger}(\mathbf{x},t)+\alpha_L^*(\mathbf{x})A(\mathbf{x},t)] \ . \tag{11}$$

By writing the LOF in the form

$$\alpha_L(\mathbf{x})=\rho_L(\mathbf{x})e^{i\phi_L(\mathbf{x})}, \quad \phi_L(\mathbf{x})=\arg[\alpha_L(\mathbf{x})]({\rm mod}\,\pi) \ , \tag{12}$$

with $\rho_L(\mathbf{x})$ real but not necessarily positive, the field E_H can be written as

$$E_H(t)=\frac{1}{N^{1/2}}\int d^2\mathbf{x}\ \rho_L(\mathbf{x})\mathscr{E}_H(\mathbf{x},t) \ , \tag{13}$$

$$\mathscr{E}_H(\mathbf{x},t)=A^{\dagger}(\mathbf{x},t)e^{i\phi_L(\mathbf{x})}+A(\mathbf{x},t)e^{-i\phi_L(\mathbf{x})} \ . \tag{14}$$

The measured quadrature depends on the LOF phase $\phi_L(\mathbf{x})$, which, in general, is not constant over the transverse plane.

Let us suppose that the quantum field $A(\mathbf{x},t)$ can be expanded on a complete orthonormal basis of functions $f_l(\mathbf{x})$, where l stands for a certain set of indices:

$$A(\mathbf{x},t)=\sum_l f_l(\mathbf{x})a_l(t) \tag{15}$$

with

$$\int d^2\mathbf{x}\ f_l^*(\mathbf{x})f_{l'}(\mathbf{x})=\delta_{l,l'} \ , \tag{16}$$

$$[a_l(t),a_{l'}^{\dagger}(t)]=\delta_{l,l'} \ . \tag{17}$$

In this case the spectrum of squeezing takes on the form

$$S(\omega)=\sum_{l,l'}\rho_l\rho_{l'}S_{l,l'}(\omega) \ , \tag{18}$$

where we have defined

$$\rho_l e^{-i\phi_l}=\frac{1}{N^{1/2}}\int d^2\mathbf{x}\ \alpha_L^*(\mathbf{x})f_l(\mathbf{x}) \tag{19}$$

and

$$S_{l,l'}(\omega)=2\gamma\int_{-\infty}^{+\infty}dt\ e^{-i\omega t}\langle:\delta A_l(t)\,\delta A_{l'}(0):\rangle \ , \tag{20}$$

$$A_l(t)=e^{i\phi_l}a_l^\dagger(t)+e^{-i\phi_l}a_l(t) \quad . \tag{21}$$

When the operators $a_l(t)$ are uncorrelated for different l, one finds

$$S_{l,l'}(\omega)=S_l(\omega,\phi_l)\,\delta_{l,l'} \quad , \tag{22}$$

where $S_l(\omega,\phi_l)$ is the single-mode spectrum of squeezing for the quadrature operator $A_l(t)$ corresponding to the particular choice of the phase ϕ_l.

We are interested in the space-time correlation function of the homodyne field $\mathscr{E}_H(\mathbf{x},t)$ defined in Eq. (14):

$$\Gamma(\mathbf{x},t;\mathbf{x}',0)=2\gamma\langle:\delta\mathscr{E}_H(\mathbf{x},t)\,\delta\mathscr{E}_H(\mathbf{x}',0):\rangle \quad . \tag{23}$$

By making use of the expansion of the quantum field over the set f_l as in Eq. (15) and assuming that these functions are real, the correlation function becomes

$$\Gamma(\mathbf{x},t;\mathbf{x}',0)=2\gamma\sum_{l,l'} f_l(\mathbf{x})f_{l'}(\mathbf{x}')\langle:\delta A_l(\mathbf{x},t)\,\delta A_{l'}(\mathbf{x}',0):\rangle \quad , \tag{24}$$

where

$$A_l(\mathbf{x},t)=e^{i\phi_L(\mathbf{x})}a_l^\dagger(t)+e^{-i\phi_L(\mathbf{x})}a_l(t) \quad . \tag{25}$$

The general expression for the correlation function simplifies under the following assumptions: (i) the phase ϕ_L of the LOF is constant over the transverse plane, so that we can write $A_l(t)$ instead of $A_l(\mathbf{x},t)$ in Eqs. (24) and (25), and (ii) the single-mode operators $a_l(t)$ are uncorrelated. Thus Eq. (24) reduces to

$$\Gamma(\mathbf{x},t;\mathbf{x}',0)=2\gamma\sum_{l} f_l(\mathbf{x})f_l(\mathbf{x}')\langle:\delta A_l(t)\,\delta A_l(0):\rangle \quad . \tag{26}$$

It is convenient to relate the space-time correlation function to the single-mode spectrum of squeezing: this can be done by inverting Eq. (20)

$$\Gamma(\mathbf{x},t;\mathbf{x}',0)=\frac{1}{2\pi}\sum_{l} f_l(\mathbf{x})f_l(\mathbf{x}')\int_{-\infty}^{+\infty}d\omega\; e^{i\omega t}S_l(\omega,\phi_L) \quad . \tag{27}$$

This formula will be applied to the case of an OPO below threshold when the functions $f_l(\mathbf{x})$ correspond to Gauss-Laguerre modes. We must remark that in such a case the correlation function is no longer the spatiotemporal Fourier transform of the spectrum of squeezing as when the field is expanded on plane waves [5]. It is straightforward to write down a similar expression for the Fourier transform

$$\tilde{\Gamma}(\mathbf{x},\mathbf{x}';\omega)=\int_{-\infty}^{+\infty}dt\; e^{-i\omega t}\Gamma(\mathbf{x},t;\mathbf{x}',0) \quad . \tag{28}$$

Under the same conditions applied in deriving Eq. (27) one finds

$$\tilde{\Gamma}(\mathbf{x},\mathbf{x}';\omega)=\sum_{l} f_l(\mathbf{x})f_l(\mathbf{x}')S_l(\omega,\phi_L) \quad . \tag{29}$$

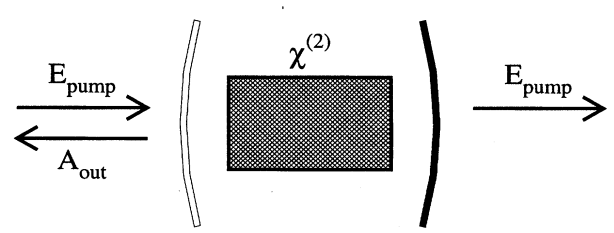

FIG. 2. Schematic view of the cavity containing a $\chi^{(2)}$ medium; the injected field E_{pump} is completely transmitted by the mirrors. A_{out} corresponds to the signal field.

III. QUANTUM MODEL FOR A DEGENERATE OPTICAL PARAMETRIC OSCILLATOR BELOW THRESHOLD

A medium with a $\chi^{(2)}$ nonlinearity is contained in a single-ended cavity with spherical mirrors (Fig. 2). The driving pump field of frequency $2\omega_s$ is converted into a signal field of frequency ω_s. We make the following assumptions: (i) the Rayleigh range of the cavity is much larger than the cavity length and (ii) the mirrors transmit completely the pump field, which is assumed to have a plane-wave configuration. Moreover, we restrict ourselves to the case in which the paraxial and the slowly varying envelope approximation and the mean-field limit are valid so that the two fields, pump and signal, are uniform along the sample in the longitudinal direction z. The cylindrical symmetry of the system around the axis of the system allows one to expand the slowly varying envelope of the signal field in terms of a set of resonator eigenmodes. In our case the suitable complete orthonormal basis is provided by the Gauss-Laguerre modes:

$$f_{pli}(r,\phi)=\frac{2}{(2^{\delta_{l,0}}\pi w^2)^{1/2}}\left[\frac{p!}{(p+l)!}\right]^{1/2}\left(2\frac{r^2}{w^2}\right)^{l/2}L_p^l\left(2\frac{r^2}{w^2}\right)\times e^{-r^2/w^2}\times\begin{cases}\cos(l\phi) & \text{for } i=1\\ \sin(l\phi) & \text{for } i=2,\end{cases} \tag{30}$$

with w being the beam waist and $p,l=0,1,2,\ldots$, respectively, the radial and the angular index. We have introduced cylindrical coordinates: $r=(x^2+y^2)^{1/2}$ represents the radial distance from the axis while ϕ denotes the angular variable in the transverse plane. The functions L_p^l are the Laguerre polynomials [16]. The modes (30) correspond to a superposition of two waves carrying, respectively, angular momenta $+l$ and $-l$; the twin photons, emitted in the process of parametric down-conversion, are associated with such waves in order to conserve the total angular momentum of radiation. The functions $f_{pli}(r,\phi)$ obey the orthonormality relation

$$\int_0^{2\pi}\int_0^{+\infty} r\,dr\,d\phi\, f_{pli}(r,\phi)f_{p'l'i'}(r,\phi)=\delta_{p,p'}\delta_{l,l'}\delta_{i,i'} \quad . \tag{31}$$

The corresponding eigenfrequencies are given by [17]

$$\omega_{pl}=\omega_{00}+(2p+l)\zeta \quad , \tag{32}$$

where ζ depends on the mirrors curvature and on the distance between them. It must be noted that the modes gather

in degenerate families, each of which is characterized by a particular value of the integer $q=2p+l$.

The quantum model for the OPO below threshold takes into account diffractive effects and is formulated in terms of a master equation describing the temporal dynamics of the intracavity field $A(\mathbf{x},t)$. According to the semiclassical treatment, the signal field in the OPO below threshold vanishes, but in a fully quantum picture there are signal photons generated by quantum noise. We neglect pump depletion and linearize the master equation around the stationary state of the OPO below threshold; hence the pump field is treated as a classical quantity. The master equation in the interaction picture reads

$$\frac{d\rho}{dt}=\frac{1}{i\hbar}[H,\rho]+\sum_{i=1,2}\sum_{p,l}\Lambda_{pli}\rho \ , \tag{33}$$

where ρ is the density operator of the intracavity signal field. The Liouvillians

$$\Lambda_{pli}=\gamma(2a_{pli}^{\dagger}\rho a_{pli}-\rho a_{pli}^{\dagger}a_{pli}-a_{pli}^{\dagger}a_{pli}\rho) \tag{34}$$

describe the damping of the mode pli due to cavity losses with rate γ. The Hamiltonian is given by

$$H=H_{\rm free}+H_{\rm int} \ , \tag{35}$$

where $H_{\rm free}$ represents the free evolution of cavity modes

$$H_{\rm free}=\hbar\sum_{i=1,2}\sum_{p,l}(\omega_{pli}-\omega_s)a_{pli}^{\dagger}a_{pli} \tag{36}$$

and the interaction Hamiltonian has the form

$$H_{\rm int}=\frac{i\hbar\gamma}{2}\mathscr{A}_p\int_0^{2\pi}\int_0^{+\infty}r\,dr\,d\phi\{[A^{\dagger}(r,\phi)]^2-[A(r,\phi)]^2\} \ , \tag{37}$$

$$\mathscr{A}_p=\frac{g}{\gamma}\mathscr{A}_s \ , \tag{38}$$

with $\mathscr{A}_s$ being the classical stationary value of the pump amplitude, which is assumed to be real and positive for simplicity. Here g is the coupling constant, proportional to the second-order susceptibility $\chi^{(2)}$. If we insert the modal expansion (15), with $f_l(\mathbf{x})$ being the Gauss-Laguerre functions, and make use of orthonormality relation (31) we obtain

$$H_{\rm int}=\frac{i\hbar\gamma}{2}\mathscr{A}_p\sum_{i=1,2}\sum_{p,l}[(a_{pli}^{\dagger})^2-a_{pli}^2] \ . \tag{39}$$

Hence the master equation describes the dynamics of an infinite set of independent, single-mode, degenerate optical parameteric oscillators. From the linear stability analysis we know [5,12] that the uniform stationary solution $\langle a_{pli}\rangle=0$ becomes unstable with respect to the buildup of a family of modes characterized by a certain value of $q=2p+l$, in correspondence to a suitable threshold value of the pump intensity $\mathscr{A}_p^2$. The value is determined by the sign of the detuning parameter

$$\Delta_{00}=\frac{\omega_{00}-\omega_s}{\gamma} \ . \tag{40}$$

When $\Delta_{00}>0$, the instability threshold corresponds to $\mathscr{A}_p^2=1+\Delta_{00}^2$ and the system emits the signal in the fundamental mode $q=0$ (i.e., $p=l=0$). When, instead, $\Delta_{00}<0$, the threshold is lower. In particular, when there is a family $2p+l=q$, which is in exact resonance with the signal field, i.e., when

$$\omega_{00}+q\zeta=\omega_s \ , \tag{41}$$

the instability arises in the modes of this family for $\mathscr{A}_p^2=1$. By using Eq. (40), condition (41) can be recast in the form

$$2p+l=-\gamma\frac{\Delta_{00}}{\zeta} \ . \tag{42}$$

IV. EQUAL TIME SPATIAL CORRELATION FUNCTION OF A GENERIC QUADRATURE COMPONENT

We are interested in the space-time behavior of the signal field purely generated by quantum noise; on average its amplitude is zero because we are considering the OPO below threshold. Hence all the information is contained in the correlation function, defined in Eq. (24). The general formalism has been described in Sec. I, so now we must only specialize it to the present case of Gauss-Laguerre modes. The space-time correlation function reads

$$\Gamma(\mathbf{x},t;\mathbf{x}',0)=2\gamma\sum_{i=1,2}\sum_{p,l}f_{pli}(r,\phi)f_{pli}(r',\phi')S_{pli}(t) \ , \tag{43}$$

where

$$S_{pli}(t)=\langle:\delta A_{pli}(t)\,\delta A_{pli}(0):\rangle \ , \tag{44}$$

and we took into account that the single-mode OPO's are uncorrelated and assumed that the LOF phase is constant over the transverse plane. This last quantity is connected through a Fourier transform to the single-mode spectrum of squeezing,

$$S_{pli}(\omega)=2\gamma\int_{-\infty}^{+\infty}dt\ e^{-i\omega t}S_{pli}(t) \ , \tag{45}$$

which is well known from the literature [18] for a single OPO. It is convenient to distinguish between the radial and the angular dependence; taking into account that the spectrum does not depend on the index i [see Eq. (48)] one has

$$\Gamma(\mathbf{x},t;\mathbf{x}',0)=2\gamma\sum_{p,l}\tilde{f}_{pl}(r)\tilde{f}_{pl}(r')\cos[l(\phi-\phi')]S_{pl}(t) \ , \tag{46}$$

with

$$\tilde{f}_{pl}(r)=\frac{2}{(2^{\delta_{l,0}}\pi w^2)^{1/2}}\left[\frac{p!}{(p+l)!}\right]^{1/2}\left(2\frac{r^2}{w^2}\right)^{l/2}\times L_p^l\left(2\frac{r^2}{w^2}\right)e^{-r^2/w^2} \ . \tag{47}$$

One notes the invariance of the space-time correlation function under rotations $\phi \to \phi + \theta$ around the axis z, which follows from the cylindrical symmetry of the system.

Now let us go further in the calculation of correlation function: we start from the spectrum of squeezing for single-mode degenerate OPO [18]

$$S_{pl}(\bar{\omega}) = \frac{4\mathscr{A}_p}{(1+\Delta_{pl}^2-\mathscr{A}_p^2-\bar{\omega}^2)^2+4\bar{\omega}^2}\{2\mathscr{A}_p+\mathrm{Re}[(1-\Delta_{pl}^2 + \mathscr{A}_p^2+\bar{\omega}^2-2i\Delta_{pl})e^{-2i\phi_L}]\} \ , \tag{48}$$

where we introduced the normalized quantities

$$\bar{\omega} = \frac{\omega}{\gamma} \ , \tag{49}$$

$$\Delta_{pl} = \frac{\omega_{pl}-\omega_s}{\gamma} = \Delta_{00} + (2p+l)\frac{\zeta}{\gamma} \ , \tag{50}$$

with Δ_{00} being defined in Eq. (40). Maximum squeezing $S_{pl}(\omega) = -1$ is predicted for the quadrature operator $i(a_{pli}^\dagger - a_{pli})$ corresponding to $\phi_L = \pi/2$: this goal is achieved at threshold for the critical modes that minimize the detuning Δ_{pl}. However, we should keep in mind that extremely close to threshold our linearized model breaks down and this result must be regarded as an asymptotic limit for the OPO below threshold. By inverting Eq. (45) we obtain the quantum fluctuations in the time domain [5]

$$S_{pl}(t) = \frac{1}{2\gamma}\frac{1}{2\pi}\int_{-\infty}^{+\infty} d\omega \ e^{i\omega t} S_{pl}(\omega) \ . \tag{51}$$

However, we should remark that this expression is valid for the field inside the cavity, because in order to deal with dimensionless quantities we introduced the factor $1/(2\gamma)$. The best intracavity squeezing is only one-half of the one achievable outside:

$$S_{pl}(\tau) = e^{-|\tau|} \times \begin{cases} (\mathscr{A}_p^2-\Delta_{pl}^2)^{-1/2}\sinh(\sqrt{\mathscr{A}_p^2-\Delta_{pl}^2}\,|\tau|)[S_{pl}(\tau=0)-\mathscr{A}_p\cos(2\phi_L)]+S_{pl}(\tau=0)\cosh(\sqrt{\mathscr{A}_p^2-\Delta_{pl}^2}\,|\tau|), & \mathscr{A}_p > |\Delta_{pl}| \\ (\Delta_{pl}^2-\mathscr{A}_p^2)^{-1/2}\sin(\sqrt{\Delta_{pl}^2-\mathscr{A}_p^2}\,|\tau|)[S_{pl}(\tau=0)-\mathscr{A}_p\cos(2\phi_L)]+S_{pl}(\tau=0)\cos(\sqrt{\Delta_{pl}^2-\mathscr{A}_p^2}\,|\tau|), & \mathscr{A}_p < |\Delta_{pl}|, \end{cases} \tag{52}$$

where $\tau = t\gamma$ and

$$S_{pl}(\tau=0) = \mathscr{A}_p \frac{\mathscr{A}_p+\cos(2\phi_L)-\Delta_{pl}\sin(2\phi_L)}{1-\mathscr{A}_p^2+\Delta_{pl}^2} \ . \tag{53}$$

By inserting the expression of $S_{pl}(\tau=0)$ into Eq. (46), one finds the equal time correlation function

$$\Gamma(\mathbf{x},\mathbf{x}';0) = 2\gamma\mathscr{A}_p\sum_{p,l}\tilde{f}_{pl}(r)\tilde{f}_{pl}(r')\cos[l(\phi-\phi')] \times \frac{\mathscr{A}_p+\cos(2\phi_L)-\Delta_{pl}\sin(2\phi_L)}{1-\mathscr{A}_p^2+\Delta_{pl}^2} \ . \tag{54}$$

We consider the special case of points $\mathbf{x}$ and $\mathbf{x}'$ having the same radial distance $r = r'$ from the axis z (i.e., they lie on the same circle of radius r); hence the correlation function (54) depends only on the angle $\Delta\phi = \phi - \phi'$. Moreover, we will discuss only the case of $\Delta_{00} \leq 0$ and will assume the resonance condition (41) between the signal field frequency ω_s and the frequency-degenerate family of modes specified by Eq. (42). Let us examine the behavior of the correlation function in the two opposite cases $\phi_L = 0$ and $\pi/2$; $\phi_L = \pi/2$ corresponds to the quadrature of maximum squeezing and $\phi_L = 0$ to the quadrature of maximum amplification.

A. Case $\phi_L = 0$

This choice corresponds to the most noisy quadrature $A^\dagger(\mathbf{x},t) + A(\mathbf{x},t)$; in such a case Eq. (53) reads

$$S_{pl}(\tau=0) = \mathscr{A}_p \frac{1+\mathscr{A}_p}{1-\mathscr{A}_p^2+\Delta_{pl}^2} \ , \tag{55}$$

and approaching threshold one finds

$$\lim_{\mathscr{A}_p \to 1-} S_{pl}(0) = \frac{2}{\Delta_{pl}^2} \ . \tag{56}$$

This result implies that for the unstable modes (for which $\Delta_{pl} = 0$) the fluctuations diverge approaching the critical point. As a consequence, the correlation function also diverges

$$\lim_{\mathscr{A}_p \to 1-} \Gamma(r,\Delta\phi) = \infty \ . \tag{57}$$

However, the ratio $\Gamma(r,\Delta\phi)/\Gamma(r,\Delta\phi=0)$ remains finite even for $\mathscr{A}_p \to 1-$ because the spatial behavior of the correlations function is determined exclusively by the unstable family of modes and the diverging factor drops:

$$\lim_{\mathscr{A}_p \to 1-} \frac{\Gamma(r,\Delta\phi)}{\Gamma(r,0)} = \frac{\Sigma'_{p,l}[\tilde{f}_{pl}(r)]^2\cos(l\Delta\phi)}{\Sigma'_{p,l}[\tilde{f}_{pl}(r)]^2} \ , \tag{58}$$

where $\Sigma'_{p,l}$ means the sum extended only to the modes of the frequency-degenerate family, which satisfies Eq. (42). Hence the angular variation arises from the factor $\cos[l(\phi-\phi')]$ of the modes that belong to the unstable family only. While the mean value of the signal field is still zero and the mean intensity is uniform over the circle, the correlation function

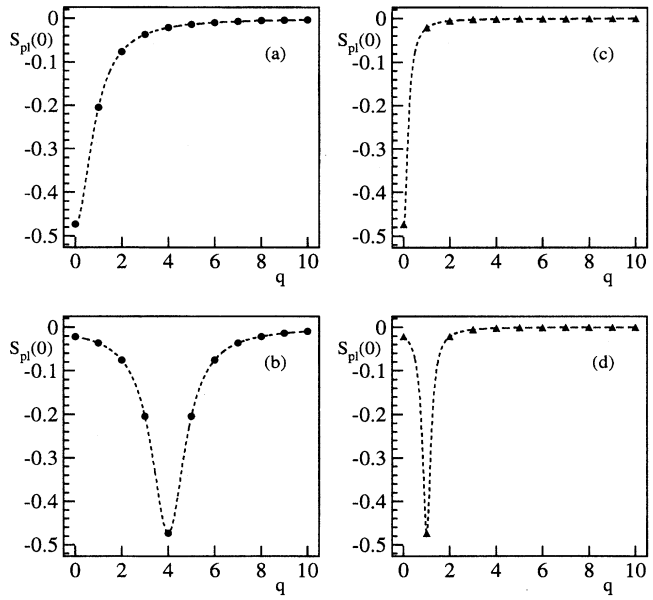

FIG. 3. Plot of equal time fluctuations $S_{pl}(\tau=0)$ of the quadrature operator $i(a_{pl}^{\dagger}-a_{pl})$ for $\mathscr{A}_p=0.9$ when (a) $\Delta_{00}=0$, $\zeta/\gamma=0.5$; (b) $\Delta_{00}=-2$, $\zeta/\gamma=0.5$; (c) $\Delta_{00}=0$, $\zeta/\gamma=2$; and (d) $\Delta_{00}=-2$, $\zeta/\gamma=2$. The markers indicate the value for each family $q=2p+l$.

displays an angular spatial modulation connected with the arising instability: such a phenomenon has been called a quantum image [4,5,19].

B. Case $\phi_L=\pi/2$

For the most squeezed quadrature one has

$$S_{pl}(\tau=0)=-\mathscr{A}_p\frac{1-\mathscr{A}_p}{1-\mathscr{A}_p^2+\Delta_{pl}^2} \quad . \tag{59}$$

In Fig. 3 we plot $S_{pl}(\tau=0)$ for $\phi_L=\pi/2$ as a function of the index $q=2p+l$, which distinguishes each family of modes, for different values of the parameters Δ_{00} [see Eq. (40)] and ζ/γ controlling the intermode spacing [cf. Eqs. (32) and (50)]. We remind here that $S_{pl}(\tau=0)$ represents the steady-state fluctuations of the intracavity field mode pl. From Figs. 3(a) and 3(b) one sees that quantum fluctuations are reduced below the shot-noise level for the family that becomes unstable at threshold ($q=0$ and 4, respectively) and for a few families around it. After increasing the intermode spacing from $\zeta/\gamma=0.5$ to 2 [Figs. 3(c) and 3(d)] the number of modes exhibiting reduced fluctuations decreases and already for $q=10$ one has $S_{pl}(\tau=0)\sim 0$. A similar result is produced when the pump field reaches the threshold value

$$\lim_{\mathscr{A}_p\to 1-} S_{pl}(\tau=0)=\begin{cases} -\frac{1}{2}, & \Delta_{pl}=0 \\ 0, & \Delta_{pl}\neq 0. \end{cases} \tag{60}$$

Hence the dominant contribution to the correlation function arises from the unstable modes family, since $S_{pl}(\tau=0)$ vanishes for the out-of-resonance modes, so that

$$\lim_{\mathscr{A}_p\to 1-}\Gamma(r,\Delta\phi)=-\gamma{\sum_{p,l}}'[\tilde{f}_{pl}(r)]^2\cos(l\Delta\phi) \quad . \tag{61}$$

It is interesting to investigate the equal time correlation function when the two points $\mathbf{x}$ and $\mathbf{x}'$ coincide because in that case one gets information about the normally ordered fluctuations of the homodyne field $\mathscr{E}_H$:

$$\Gamma(r,\Delta\phi=0)=2\gamma\langle:[\delta\mathscr{E}_H(r,\phi,t)]^2:\rangle \quad , \tag{62}$$

as it follows from Eq. (23). Through Eq. (27) it is possible to link the properties of the correlation function to those of single-mode spectrum of squeezing:

$$\Gamma(r,\Delta\phi=0)=\frac{1}{2\pi}{\sum_{p,l}}[\tilde{f}_{pl}(r)]^2\int_{-\infty}^{+\infty}d\omega\ S_{pl}(\omega) \quad . \tag{63}$$

The negativity of the correlation function reflects the nonclassical effect of squeezing in the output field (i.e., $S_{pl}<0$) in the quadrature under consideration; hence it is a signature of the quantum nature of the fluctuations that generate the signal field below threshold. We point out that even at threshold the correlation function remains negative thanks to the contribution of the unstable family of modes:

$$\lim_{\mathscr{A}_p\to 1-}\Gamma(r,\Delta\phi=0)=-\gamma{\sum_{p,l}}'[\tilde{f}_{pl}(r)]^2 \quad . \tag{64}$$

On the contrary, in the case of the OPO with plane mirrors, analyzed in [5], one deals with a continuum of modes: this means that the sum is replaced by an integral and upon approaching threshold the bandwidth of modes with relevant noise reduction shrinks to a single point so that the correlation function vanishes and the influence of squeezing disappears.

We note that despite the noteworthy difference between Eqs. (61) and (57), the ratio $\Gamma(r,\Delta\phi)/\Gamma(r,0)$ for $\phi_L=\pi/2$ approaches the same limit (58) obtained for $\phi_L=0$, when $\mathscr{A}_p\to 1-$. Actually, the limit (58) holds for any value of the phase ϕ_L. Incidentally, it happens that the ratio $\Gamma(r,\Delta\phi)/\Gamma(r,0)$ takes on the same value for $\phi_L=0$ and $\pi/2$ also far from threshold. In fact, the squeezing spectra in the two cases turn out to be proportional:

$$S_{pl}(\tau=0,\phi_L=0)=\frac{\mathscr{A}_p+1}{\mathscr{A}_p-1}S_{pl}(\tau=0,\phi_L=\pi/2) \quad . \tag{65}$$

Because the proportionality factor is independent of the indices p and l, it can be simplified in the expression of the ratio, which gives equal results for both quadrature components. This property is no longer true for two arbitrary phases of the local oscillator field.

V. NUMERICAL EXAMPLES

We have calculated the equal time correlation function given by Eq. (54), by truncating the sum to a large but finite value (100) of indices p and l. We believe that this numerical restriction does not affect the results; moreover, real systems cannot support transverse modes of arbitrary high order because of diffraction losses related to the finite size of mirrors and of other intracavity elements, such as pinholes and modulators. As a first example, we consider the case

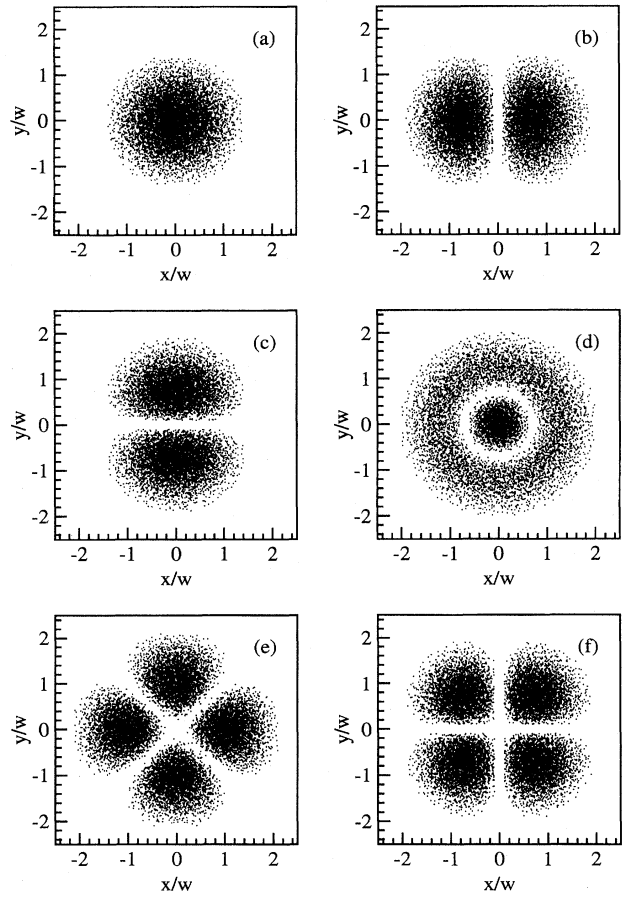

FIG. 4. Intensity profiles in the transverse plane of the three first families of modes $q=0$, 1, and 2: (a) fundamental mode TEM_{00}; (b) and (c) mode (0,1) with $i=1,2$, respectively; (d) mode (1,0); and (e) and (f) mode (0,2) with $i=1,2$, respectively.

($\Delta_{00}=0$) in which the instability arises in the fundamental mode (0,0), usually designated as TEM_{00}:

$$f_{00}(r)=\left(\frac{2}{\pi w^2}\right)^{1/2} e^{-r^2/w^2} \quad . \tag{66}$$

Its intensity profile, characterized by cylindrical symmetry, is shown in Fig. 4(a). We are interested in the angular dependence of correlation function, measured between two points on the same circle, and in order to exhibit the spatial modulation in the best way it is convenient to plot the ratio $\Gamma(r,\Delta\phi)/\Gamma(r,0)$. This quantity has been evaluated for both quadratures $\phi_L=0$ and $\pi/2$ and we found that in any case one obtains the same results even though, as pointed out in Sec. IV, the two operators are affected by quantum noise in a completely different way. In Fig. 5 we plot this ratio for different values of the pump field amplitude. Far from threshold (solid line), the correlation decreases substantially away from the value $\Delta\phi=0,2\pi$. Approaching threshold (dashed line), the correlation increases everywhere and becomes perfectly constant at threshold (dotted line) because the contribution of the ϕ-independent fundamental mode is dominant. Thus there is a perfect correlation over the whole

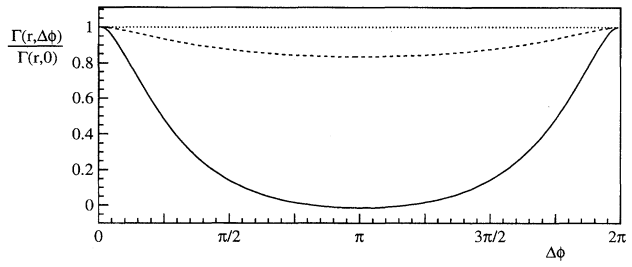

FIG. 5. Ratio $\Gamma(r,\Delta\phi)/\Gamma(r,\Delta\phi=0)$ plotted along a circumference of radius $r=w$, when $\Delta_{00}=0$, $\phi_L=0,\pi/2$, and $\zeta/\gamma=1$ for increasing values of pump amplitude: $\mathscr{A}_p=0.5$ (solid line), $\mathscr{A}_p=0.9$ (dashed line), and $\mathscr{A}_p=1$ (dotted line).

circle and this behavior is the analog, in the case of spherical mirrors, of the divergence of the correlation length found in the case of planar mirrors [5]. An increase of the intermode spacing ζ/γ produces the same effect on the ratio $\Gamma(r,\Delta\phi)/\Gamma(r,0)$ as approaching threshold, i.e., the out-of-resonance modes are less effective and spatial modulations tend to disappear. Also in the following cases it remains true that the increase of the ratio ζ/γ enhances the contribution of the mode family resonant with the signal field.

Let us now turn to examine the case when $\Delta_{00}<0$ and the instability arises in $q=1$, because Eq. (42) is satisfied for $2p+l=1$. Figures 4(b) and 4(c) show, respectively, the intensity profiles of the cosine mode (f_{011}) and of the sine mode (f_{012}) in the transverse plane; the correlation function is computed on the circle where their intensity is maximum. The curves in Fig. 6 describe the behavior of the ratio $\Gamma(r,\Delta\phi)/\Gamma(r,0)$ as a function of the relative angle $\Delta\phi$ between the two points $\mathbf{x}$ and $\mathbf{x}'$ in which the spatial correlation function is calculated. Again, by increasing the pump amplitude from 0.5 (solid line) to threshold (dotted line) one observes that the unstable family plays a more and more important role. In particular, the oscillations at threshold agree with the prediction of Eq. (58) when $l=1$

$$\lim_{\mathscr{A}_p\to -} \frac{\Gamma(\Delta\phi)}{\Gamma(0)}=\cos(\phi-\phi') \quad . \tag{67}$$

As anticipated in Sec. IV, the correlation function exhibits an ordered spatial modulation despite the fact that the mean

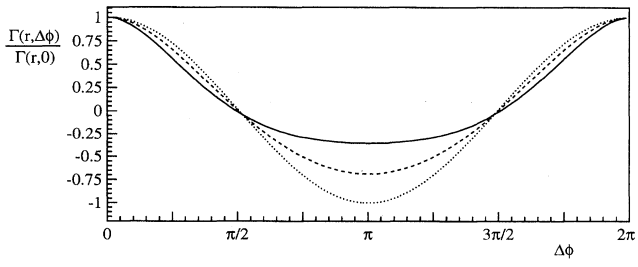

FIG. 6. Ratio $\Gamma(r,\Delta\phi)/\Gamma(r,\Delta\phi=0)$ plotted along a circumference of radius $r=w/\sqrt{2}$, where the intensity of unstable modes f_{011} and f_{012} has a maximum. The detuning parameter is $\Delta_{00}=-1$, $\phi_L=0,\pi/2$, $\zeta/\gamma=1$, and the pump amplitude $\mathscr{A}_p$ is equal to 0.5 (solid line), 0.9 (dashed line), and threshold (dotted line).

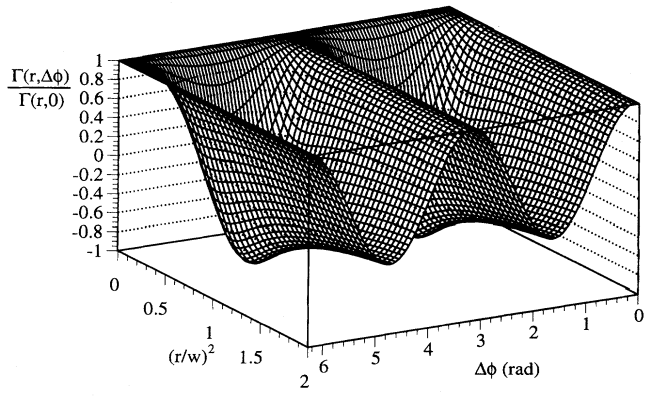

FIG. 7. Three-dimensional plot of $\Gamma(r,\Delta\phi)/\Gamma(r,0)$ as a function of r, the radius of the circle along which the correlation function is calculated, and $\Delta\phi$, the relative angle between $\mathbf{x}$, and $\mathbf{x}'$. The pump amplitude is equal to threshold; $\Delta_{00}=-2$, $\zeta/\gamma=1$, and $\phi_L=0,\pi/2$.

intensity of the signal field in the stationary state is uniform over the circle. The field possesses a spatial structure that can be investigated through the correlation function; hence the system provides an example of a quantum image [5].

As a final example we investigate the case of $q=2$, where there is degeneracy with respect to three distinct Gauss-Laguerre modes: $p=1$, $l=0$ and $p=0$, $l=2$ (sine and cosine configurations). The intensities of those modes are plotted in Fig. 4: one sees that the intensity of mode (1,0) presents a central peak surrounded by a ring, while a linear combination of cosine and sine modes (0,2) gives rise to a doughnut mode. Varying the radius of the circle on which the correlation function is measured, the ratio $\Gamma(r,\Delta\phi)/\Gamma(r,0)$ reflects the changes in the intensity of modes under consideration. Figure 7 presents the ratio $\Gamma(r,\Delta\phi)/\Gamma(r,0)$ as a function of the relative angle $\Delta\phi$ and of the radius of the circle. Since we are at threshold, the behavior of the correlation function is dominated by the modes of the resonant family; in particular, at $r=w/\sqrt{2}$ the intensity of mode $p=1$, $l=0$ vanishes and hence the ratio $\Gamma(r,\Delta\phi)/\Gamma(r,0)$ oscillates as $\cos[2(\phi-\phi')]$. This is clearer from Fig. 8, where the same quantity is measured over the circle with radius $r=w/\sqrt{2}$ for different values of pump amplitude. The mode $p=1$, $l=0$ does not contribute and the spatial modulation is due exclu-

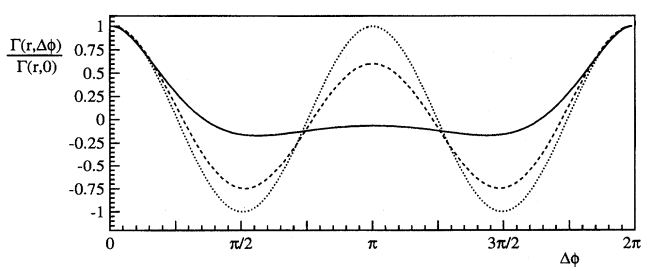

FIG. 8. Ratio $\Gamma(r,\Delta\phi)/\Gamma(r,\Delta\phi=0)$ plotted along the circle with radius $r=w/\sqrt{2}$. The detuning is $\Delta_{00}=-1$, $\zeta/\gamma=0.5$, and $\phi_L=0,\pi/2$; $\mathscr{A}_p=0.5$ (solid line), $\mathscr{A}_p=0.99$ (dashed line), and $\mathscr{A}_p$ equal to threshold (dotted line).

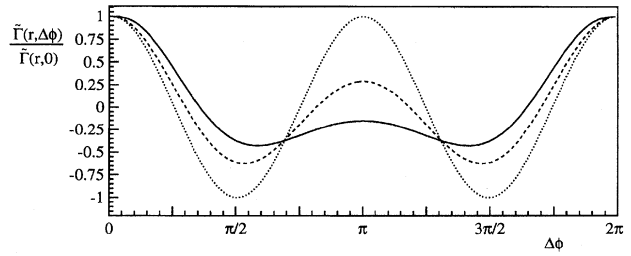

FIG. 9. Spatial correlation function $\tilde{\Gamma}(r,\Delta\phi)$ normalized to $\tilde{\Gamma}(r,\Delta\phi=0)$ vs the angular difference $\Delta\phi$ along a circle of radius $r=w/\sqrt{2}$. The detuning is $\Delta_{00}=-1$, $\zeta/\gamma=0.5$, and $\phi_L=0$; $\mathscr{A}_p=0.5$ (solid line), $\mathscr{A}_p=0.9$ (dashed line), and $\mathscr{A}_p$ equal to threshold (dotted line).

sively to the other unstable modes f_{021} and f_{022}. Far from threshold (solid line) the correlation decays rapidly with the angular distance between the two points $\mathbf{x}$ and $\mathbf{x}'$. Close to threshold (dashed line) the correlation length increases and a spatial structure, which becomes a perfect sinusoidal oscillation at threshold (dotted line), emerges; this corresponds again to a quantum image. Again, at threshold the correlation extends to the whole circumference; this phenomenon for our system with cylindrical symmetry corresponds to the critical divergence of the correlation length in the system with translational invariance, considered in [5].

VI. SPATIAL CORRELATION FUNCTION IN THE FREQUENCY DOMAIN

It is worthwhile to investigate the spatial properties of the correlation function in the frequency domain also in view of possible experimental implementations. The general form of the Fourier transform of the correlation function is found at the end of Sec. II [Eq. (29)]; in the case of Gauss-Laguerre modes it reads

$$\tilde{\Gamma}(\mathbf{x},\mathbf{x}';\bar{\omega})=\sum_{i=1,2}\sum_{p,l} f_{pli}(\mathbf{x})f_{pli}(\mathbf{x}')S_{pl}(\bar{\omega}) \quad , \tag{68}$$

where we recall that $\bar{\omega}=\omega/\gamma$ and the expression of the spectrum of squeezing is given by Eq. (48). We analyze separately the zero-frequency behavior of the correlation function for the two quadrature operators corresponding to LOF phases $\phi_L=0,\pi/2$.

A. Case $\phi_L=0$

Approaching threshold for signal generation, the spectrum $S_{pl}(\bar{\omega}=0)$ diverges in correspondence with the unstable modes; the situation is therefore analogous to what happens in the time domain [see Eq. (56)]. The conclusions of Sec. IV A apply equally well to the present case and, again, the ratio $\tilde{\Gamma}(\mathbf{x},\mathbf{x}';\bar{\omega}=0)/\tilde{\Gamma}(\mathbf{x}=\mathbf{x}';\bar{\omega}=0)$ remains finite, displaying a spatial structure determined by the unstable family of modes. A nice example of quantum image is provided by Fig. 9, where, as usual, the correlation function is calculated between two points lying on the same circle; the curves correspond to different values of pump amplitude $\mathscr{A}_p$ ranging from 0.5 to threshold. The family $q=2$ is on resonance and at threshold the correlation function displays a perfect sinu-

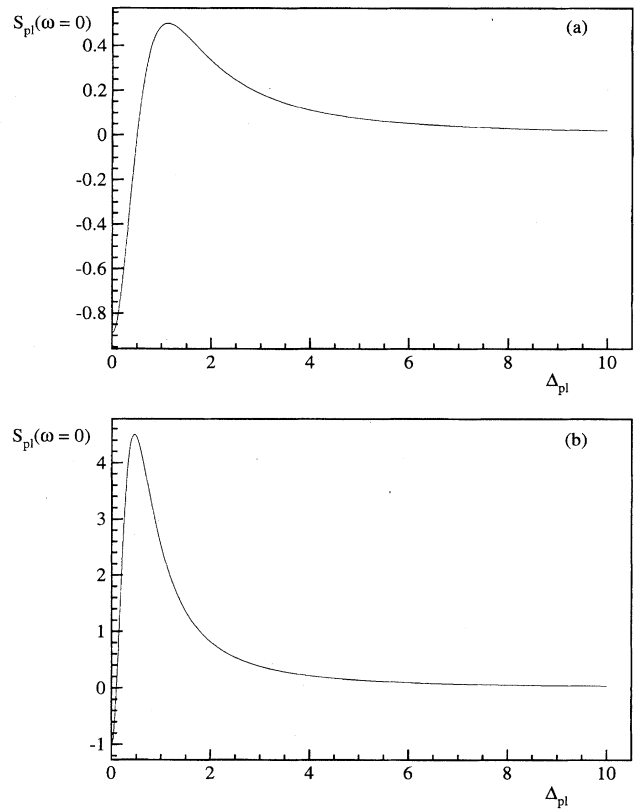

FIG. 10. Plot of the zero-frequency spectrum of squeezing $S_{\rm pl}$ of the quadrature operator $i(a_{pl}^{\dagger}-a_{pl})$ vs the detuning $\Delta_{\rm pl}$: (a) $\mathscr{A}_p=0.5$ and (b) $\mathscr{A}_p=0.9$.

soidal oscillation along the whole circumference. The picture is quite similar to that of the equal time correlation function (Fig. 8).

B. Case $\phi_L=\pi/2$

When the phase ϕ_L is equal to $\pi/2$, the spectrum of squeezing at zero frequency turns out to be

$$S_{pl}(\bar{\omega}=0)=\frac{4\mathscr{A}_p}{(1-\mathscr{A}_p^2+\Delta_{pl}^2)^2}[\Delta_{pl}^2-(1-\mathscr{A}_p)^2] \quad (69)$$

and is plotted in Fig. 10 as a function of the detuning Δ_{pl} for two different values of the pump amplitude: (a) $\mathscr{A}_p=0.5$ and (b) $\mathscr{A}_p=0.9$. It is evident that increasing the pump the maximum increases and moves closer to $\Delta_{pl}=0$, even though at threshold one has complete noise suppression $S_{pl}(\bar{\omega}=0)=-1$ for the unstable modes ($\Delta_{pl}=0$). Unlike the case of the equal time correlation function $S_{pl}(\tau=0)$, which is always negative, for $\phi_L=\pi/2$ here the squeezing effect $S_{pl}(\bar{\omega}=0)<0$ is restricted to a small bandwidth of modes around the unstable family, which shrinks as the pump amplitude approaches threshold. The large maximum plays a fundamental role in the Fourier transform of the correlation function because now the leading terms are not only those corresponding to the unstable modes but also other modes sufficiently close to resonance. In Fig. 11 we plot the ratio $\tilde{\Gamma}(r,\Delta\phi)/\tilde{\Gamma}(r,0)$ when the resonance condition is met

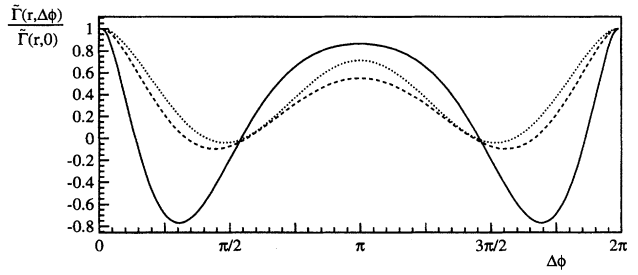

FIG. 11. Plot of the ratio $\tilde{\Gamma}(r,\Delta\phi)/\tilde{\Gamma}(r,\Delta\phi=0)$ along a circle of radius $r=w/\sqrt{2}$ for $\phi_L=\pi/2$, $\Delta_{00}=-0.5$, and $\zeta/\gamma=0.5$; $\mathscr{A}_p=0.5$ (solid line), $\mathscr{A}_p=0.9$ (dashed line), and $\mathscr{A}_p$ equal to threshold (dotted line).

by the family $q=1$; however, the spatial modulation at threshold is different from $\cos(\phi-\phi')$, which we found in the equal time correlation function for the same set of parameters, because of the contribution from nonresonant modes.

VII. CORRELATION FUNCTION OF INTENSITY FLUCTUATIONS

An alternative approach to investigate spatial structures of a field generated by quantum noise is provided by the correlation function of intensity fluctuations. This method is simpler from an experimental point of view because it does not require a local oscillator field. We define the correlation function

$$\Gamma^{(2)}(\mathbf{x},t;\mathbf{x}',t')=\langle \delta I_{\rm out}(\mathbf{x},t)\,\delta I_{\rm out}(\mathbf{x}',t')\rangle \ , \quad (70)$$

where

$$\delta I_{\rm out}(\mathbf{x},t)=I_{\rm out}(\mathbf{x},t)-\langle I_{\rm out}\rangle \ . \quad (71)$$

$I_{\rm out}(\mathbf{x},t)$ is the intensity of the output signal field measured at time t and at the position $\mathbf{x}=(x,y)$. In terms of field operators Eq. (70) turns out to be

$$\Gamma^{(2)}(\mathbf{x},t;\mathbf{x}',t')=\langle I_{\rm out}(\mathbf{x},t)\rangle\,\delta(\mathbf{x}-\mathbf{x}')\,\delta(t-t') + G^{(2)}(\mathbf{x},t;\mathbf{x}',t') \ , \quad (72)$$

$$G^{(2)}(\mathbf{x},t;\mathbf{x}',t')=\langle A_{\rm out}^{\dagger}(\mathbf{x},t)A_{\rm out}^{\dagger}(\mathbf{x}',t')A_{\rm out}(\mathbf{x}',t')A_{\rm out}(\mathbf{x},t)\rangle - \langle I_{\rm out}(\mathbf{x},t)\rangle\langle I_{\rm out}(\mathbf{x}',t')\rangle \ . \quad (73)$$

The first term is the shot-noise contribution and is proportional to the mean intensity, as usual. The second one $G^{(2)}(\mathbf{x},t;\mathbf{x}',t')$ corresponds to the normally ordered part and, according to quantum detection theory [20], represents the intensity correlation function. The calculation of $G^{(2)}(\mathbf{x},t;\mathbf{x}',t')$ is carried out in the Appendix.

Since we are much more interested in the spatial properties of the signal field rather than in its temporal behavior, we consider the special case of equal time correlation function, as we did previously for the quadrature operators. By expanding the field on the basis of Gauss-Laguerre modes, we arrive at the result

$$G^{(2)}(\mathbf{x},\mathbf{x}')=\gamma^2\left|\sum_{i=1,2}\sum_{p,l} f_{pli}(\mathbf{x})f_{pli}(\mathbf{x}')\frac{\mathscr{A}_p(1+i\Delta_{pl})}{1-\mathscr{A}_p^2+\Delta_{pl}^2}\right|^2 + \gamma^2\left[\sum_{i=1,2}\sum_{p,l} f_{pli}(\mathbf{x})f_{pli}(\mathbf{x}')\frac{\mathscr{A}_p^2}{1-\mathscr{A}_p^2+\Delta_{pl}^2}\right]^2 . \quad (74)$$

Again, the expression above can be cast in such way that the cylindrical symmetry becomes apparent

$$G^{(2)}(\mathbf{x},\mathbf{x}')=\gamma^2\left|\sum_{p,l}\tilde{f}_{pl}(r)\tilde{f}_{pl}(r')\cos(l\Delta\phi)\frac{\mathscr{A}_p(1+i\Delta_{pl})}{1-\mathscr{A}_p^2+\Delta_{pl}^2}\right|^2 + \gamma^2\left[\sum_{p,l}\tilde{f}_{pl}(r)\tilde{f}_{pl}(r') \times\cos(l\Delta\phi)\frac{\mathscr{A}_p^2}{1-\mathscr{A}_p^2+\Delta_{pl}^2}\right]^2 , \quad (75)$$

where the functions $\tilde{f}_{pl}(r)$ are given in Eq. (47) and $\Delta\phi=\phi-\phi'$. We note that the correlation function never takes negative values; this phenomenon is linked to photon bunching in the time domain and is a signature of increased intensity fluctuations. Indeed, fluctuations diverge at threshold for signal generation for the unstable modes, which meet the resonance condition $\Delta_{pl}=0$; this means that the correlation function is dominated by the particular family of modes $q=2p+l$, which satisfies condition (42).

In Fig. 12(a) we plot the normally ordered correlation function of the intensity fluctuations near threshold ($\mathscr{A}_p=0.999$), when the instability arises in the family $q=2$, corresponding to the modes $p=0$, $l=2$, with $i=1,2$, and $p=1$, $l=0$. We fixed the point $\mathbf{x}$ so that the mode $p=1$, $l=0$ vanishes and varied the second point $\mathbf{x}'$ in the transverse plane; this choice enhances the oscillatory character of the spatial correlation function, suppressing the unmodulated contribution coming from the mode $p=1$, $l=0$. The resulting pattern exhibits, as expected, a modulation as $\cos^2(2\Delta\phi)$. In general, an arbitrary location of the point $\mathbf{x}$ reduces the symmetry because of the interplay of the on-resonance modes [see Fig. 12(b)]. If we restrict the analysis to a circle, along which the mode $p=1$, $l=0$ is zero, we obtain the oscillating behavior shown in Fig. 13, similar to the plots obtained for quadrature operators.

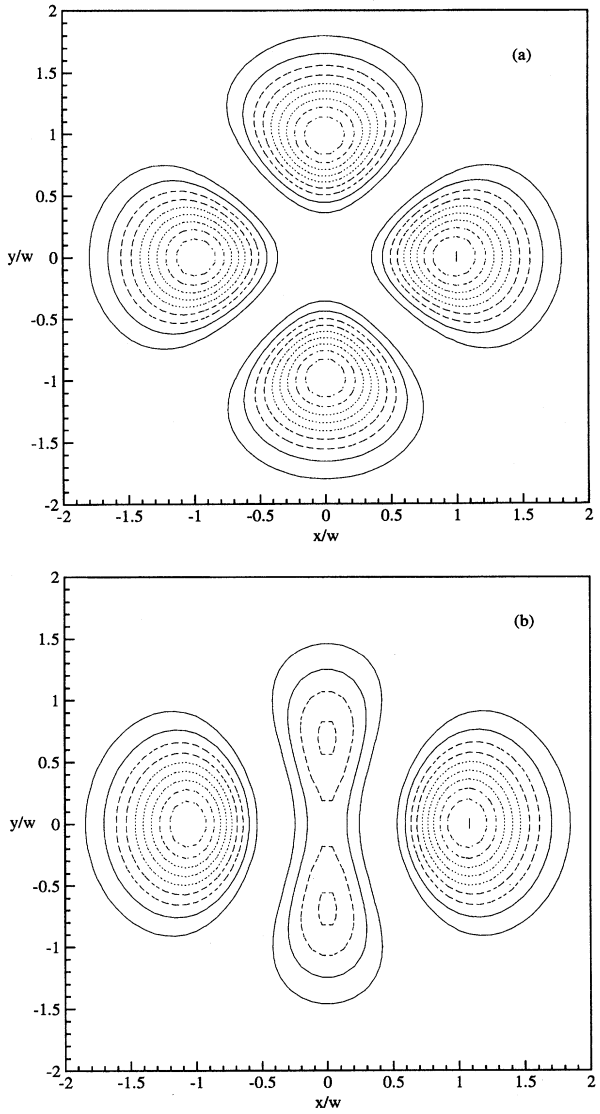

FIG. 12. Contour plot of equal time correlation function $G^{(2)}(\mathbf{x},\mathbf{x}')$ where (a) $\mathbf{x}=(w/\sqrt{2},0)$ and (b) $\mathbf{x}=(w,0)$ and $\mathbf{x}'$ varies in the transverse plane. The detuning is $\Delta_{00}=-2$, the pump amplitude is $\mathscr{A}_p=0.999$, and $\zeta/\gamma=1$.

VIII. CORRELATION FUNCTION OF INTENSITY FLUCTUATIONS IN THE FREQUENCY DOMAIN

To complete the analysis of spatial properties of the signal field, we calculate also the correlation function of the intensity fluctuations in the frequency domain. In general, the spectrum of intensity fluctuations is defined as

$$S^{(2)}(\mathbf{x},\mathbf{x}';\Omega)=\int_{-\infty}^{+\infty}dt\; e^{i\Omega t}\langle\delta I_{\rm out}(\mathbf{x},t)\,\delta I_{\rm out}(\mathbf{x}',0)\rangle = \delta(\mathbf{x}-\mathbf{x}')\langle I_{\rm out}\rangle+\tilde{G}^{(2)}(\Omega) \quad , \quad (76)$$

$$\tilde{G}^{(2)}(\mathbf{x},\mathbf{x}';\Omega)=\int_{-\infty}^{+\infty}dt\; e^{i\Omega t}G^{(2)}(\mathbf{x}',0;\mathbf{x},t) \quad , \quad (77)$$

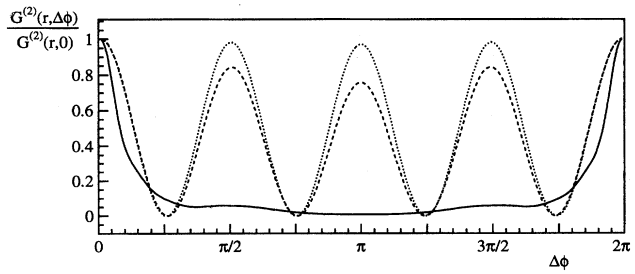

FIG. 13. Ratio $G^{(2)}(r,\Delta\phi)/G^{(2)}(r,0)$ plotted along a circle of radius $r=w/\sqrt{2}$. The detuning parameter is $\Delta_{00}=-2$, $\zeta/\gamma=1$, and the pump amplitude $\mathscr{A}_p$ is equal to 0.5 (solid line), 0.99 (dashed line), and 0.999 (dotted line).

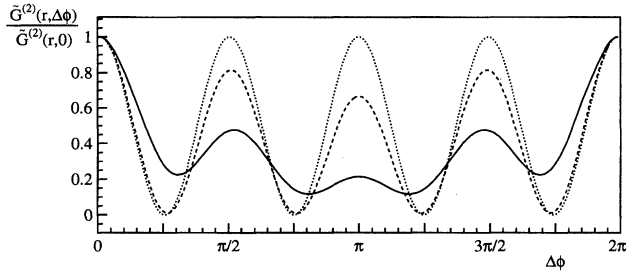

FIG. 14. Ratio $\tilde{G}^{(2)}(r,\Delta\phi)/\tilde{G}^{(2)}(r,0)$ plotted along a circle of radius $r=w/\sqrt{2}$. The other parameters are $\Delta_{00}=-2$, $\zeta/\gamma=1$, and the pump amplitude $\mathscr{E}_p$ is equal to 0.5 (solid line), 0.9 (dashed line), and 0.999 (dotted line). The curve for $\mathscr{E}_p=0.99$ is practically indistinguishable from the dotted line.

where we separated the shot-noise contribution from the Fourier transform $\tilde{G}^{(2)}(\mathbf{x},\mathbf{x}';\Omega)$, of the normally ordered part defined by Eq. (73), which carries the interesting information concerning the spatial behavior. In the simplest case of zero frequency, we have been able to find an analytical expression, which is, however, quite involved. Therefore, we present here only the results of the numerical implementation of such that allow for readily capturing the main features. In analogy to Sec. VII, Fig. 14 shows the zero-frequency spectrum of the normally ordered correlation function along a circle of radius $r=w/\sqrt{2}$ when the family of modes $q=2$ matches the resonance condition (41). It is remarkable that approaching threshold the spectrum of the correlation function displays an increasing spatial order, characterized by a sinusoidal modulation, which in the case under consideration corresponds to the function $\cos^2(2\Delta\phi)$. This implies that also in the frequency domain the phenomenon of quantum images is present and the pattern, "visible" through the Fourier transform of the time correlation function, is again connected to the family of modes that becomes unstable at threshold.

IX. CONCLUSIONS

In this paper we have, first of all, extended the results of [5] to the realistic case of cavity with spherical mirrors, in which one has only cylindrical symmetry, whereas for the cavity with plane mirrors considered in [5] there was both translational and rotational symmetry. With this proviso, all the interesting phenomena pointed out in [5] basically remain valid in the case of cavity with spherical mirrors, namely, we showed the following.

(i) Approaching threshold, all the points of an arbitrary circle centered at the axis of the system become perfectly correlated and this is analog of the divergence of the correlation length found in the case of translational symmetry.

(ii) When the detuning parameter Δ_{00} is negative, the correlation function exhibits a sinusoidal modulation over the circle. Because the mean intensity is uniform along the circle, this means that one has again the quantum image phenomenon.

(iii) For the "squeezed" quadrature component, the value of the correlation function calculated for equal points is negative, which demonstrates the quantum nature of the fluctuations that generate the signal field. This feature is true for the equal time correlation function, but not for the zero-frequency correlation function.

In addition to the spatial correlation function of a generic quadrature component, we have also calculated the more easily measurable spatial correlation function of the intensity fluctuations, both for equal times and for zero frequency. The same properties (i) and (ii) hold also for this correlation function, whereas property (iii) is not true even for the equal time case; the latter fact is related to the absence of antibunching in the squeezed vacuum state.

In this work we aimed to provide a simple but realistic model that can lend itself to experimental implementation. To proceed in this direction one might drop the hypothesis of a plane-wave-injected field, replacing it with a Gaussian beam both in the case considered here and for a system without cavity, which generates squeezed light by means of a traveling wave interacting with a nonlinear crystal [21]. We trust that the extension to the case of a cavity with spherical mirrors and to intensity correlation function, obtained in this paper, can pave the way to the experimental observation of the described phenomena.

ACKNOWLEDGMENTS

We are grateful to A. Gatti for her precious collaboration and to G. Leuchs for a stimulating discussion. This research has been carried out in the framework of the ESPRIT Long Term Research Project No. 6934 QUINTEC and of the Human Capital and Mobility Network 920887 "Nonclassical Light."

APPENDIX

In order to compute the second-order correlation function

$$G^{(2)}(\mathbf{x},t;\mathbf{x}',t')$$
$$=\langle A^{\dagger}_{\rm out}(\mathbf{x},t)A^{\dagger}_{\rm out}(\mathbf{x}',t')A_{\rm out}(\mathbf{x}',t')A_{\rm out}(\mathbf{x},t)\rangle$$
$$-\langle A^{\dagger}_{\rm out}(\mathbf{x},t)A_{\rm out}(\mathbf{x},t)\rangle\langle A^{\dagger}_{\rm out}(\mathbf{x}',t')A_{\rm out}(\mathbf{x}',t')\rangle \quad \text{(A1)}$$

it is convenient to relate the output field $A_{\rm out}(\mathbf{x},t)$ to the input field $A_{\rm in}(\mathbf{x},t)$, which in our case is in the vacuum state. To this end, we follow the approach of Langevin equations [15] for the slowly varying envelope field operator inside the cavity

$$\frac{\partial A}{\partial t}(\mathbf{x},t)=-\gamma\Big[(1+i\Delta_{00})A(\mathbf{x},t)-\mathscr{E}_pA^{\dagger}(\mathbf{x},t)$$
$$-i\frac{\zeta}{\gamma}\left(1-\frac{r^2}{w^2}+\frac{w^2}{4}\nabla_{\perp}^2\right)A(\mathbf{x},t)\Big]$$
$$+\sqrt{2\gamma}A_{\rm in}(\mathbf{x},t)\ , \quad \text{(A2)}$$

where $\nabla_{\perp}^2=\partial^2/\partial x^2+\partial^2/\partial y^2$ is the transverse Laplacian and $A_{\rm in}(\mathbf{x},t)$ represents the noise term, i.e., the vacuum input entering the cavity through the outcoupling mirror. By inserting the field expansion (15) in the Eq. (A2) and by projecting onto the Gauss-Laguerre modes and taking into account the relation [22]

$$\left[\frac{w^2}{4}\nabla_\perp^2-\left(\frac{r}{w}\right)^2\right]f_{pli}(r,\phi)=-(2p+l+1)f_{pli}(r,\phi) \quad , \tag{A3}$$

we obtain

$$\frac{\partial a_{pli}}{\partial t}(t)=-\gamma[(1+i\Delta_{pl})a_{pli}(t)-\mathscr{A}_p a_{pli}^\dagger(t)] + \sqrt{2\gamma}a_{pli}^{\rm in}(t) \quad , \tag{A4}$$

with

$$A_{\rm in}(\mathbf{x},t)=\sum_{i=1,2}\sum_{p,l} f_{pli}(r,\phi)a_{pli}^{\rm in}(t) \tag{A5}$$

and Δ_{pli} given by Eq. (50). The equation above, together with the one for $a_{pli}^\dagger(t)$, forms a linear system that can be easily solved in the frequency domain. Let us define the Fourier transforms

$$a_{pli}(\Omega)=\int_{-\infty}^{+\infty} dt\ e^{i\Omega t}a_{pli}(t) \quad , \tag{A6}$$

$$a_{pli}^\dagger(-\Omega)=\int_{-\infty}^{+\infty} dt\ e^{i\Omega t}a_{pli}^\dagger(t) \quad . \tag{A7}$$

If we take into account that the output field is linked to the input and intracavity fields by the relation

$$a_{pli}^{\rm out}(\Omega)=\sqrt{2\gamma}a_{pli}(\Omega)-a_{pli}^{\rm in}(\Omega) \quad , \tag{A8}$$

where $a_{pli}^{\rm out}(\Omega)$ and $a_{pli}^{\rm in}(\Omega)$ are defined in an obvious way, we find for each mode

$$a_{pli}^{\rm out}(\omega)=U_{pl}(\omega)a_{pli}^{\rm in}(\omega)+V_{pl}(\omega)a_{pli}^{\dagger\,\rm in}(-\omega) \quad , \tag{A9}$$

where the coefficients of the unitary transformation are

$$U_{pl}(\omega)=\frac{[1-i\Delta_{pl}(-\omega)][1-i\Delta_{pl}(\omega)]+\mathscr{A}_p^2}{[1+i\Delta_{pl}(\omega)][1-i\Delta_{pl}(-\omega)]-\mathscr{A}_p^2} \quad , \tag{A10}$$

$$V_{pl}(\omega)=\frac{2\mathscr{A}_p}{[1+i\Delta_{pl}(\omega)][1-i\Delta_{pl}(-\omega)]-\mathscr{A}_p^2} \quad . \tag{A11}$$

Here we introduced the dimensionless frequency $\omega=\Omega/\gamma$, while $\Delta_{pl}(\pm\omega)=\Delta_{pl}\mp\omega$, where the upper and lower signs must be taken concurrently. The input-output relation (A9) together with commutation rule

$$[a_j^{\rm in}(\Omega),a_k^{\dagger\,\rm in}(\Omega')]=2\pi\delta_{j,k}\delta(\Omega-\Omega') \tag{A12}$$

enables us to compute the output field correlation functions of any arbitrary order. For simplicity, we use in (A12) and in the following a single label i (or j, k, or l), which stands for the whole set of indices $\{pli\}$. In particular, the second-order correlation function turns out to be given by

$$\begin{aligned}&\langle a_i^{\dagger\,\rm out}(\Omega_1)a_j^{\dagger\,\rm out}(\Omega_2)a_k^{\rm out}(\Omega_3)a_l^{\rm out}(\Omega_4)\rangle \\ &=(2\pi)^2\{\delta_{i,j}\delta_{k,l}\delta(\Omega_1+\Omega_2)\delta(\Omega_3+\Omega_4)V_i^*(\Omega_1)U_j^*(\Omega_2)U_k(\Omega_3)V_l(\Omega_4)+[\delta_{i,k}\delta_{j,l}\delta(\Omega_1-\Omega_3)\delta(\Omega_2-\Omega_4) \\ &\quad+\delta_{i,l}\delta_{j,k}\delta(\Omega_1-\Omega_4)\delta(\Omega_2-\Omega_3)]V_i^*(\Omega_1)V_j^*(\Omega_2)V_k(\Omega_3)V_l(\Omega_4)\} \ ;\end{aligned} \tag{A13}$$

this result holds for a vacuum input, in which case normally ordered quantities have a vanishing expectation value. With an inverse Fourier transform and by summing up over Gauss-Laguerre modes, we obtain the equal time intensity correlation function of signal field

$$G^{(2)}(\mathbf{x},\mathbf{x}')=\gamma^2\left|\sum_{i=1,2}\sum_{p,l} f_{pli}(\mathbf{x})f_{pli}(\mathbf{x}')\frac{\mathscr{A}_p(1+i\Delta_{pl})}{1-\mathscr{A}_p^2+\Delta_{pl}^2}\right|^2+\gamma^2\left[\sum_{i=1,2}\sum_{p,l} f_{pli}(\mathbf{x})f_{pli}(\mathbf{x}')\frac{\mathscr{A}_p^2}{1-\mathscr{A}_p^2+\Delta_{pl}^2}\right]^2 \quad . \tag{A14}$$

[1] See, for example, L. A. Lugiato, Chaos Solitons Fractals **4**, 1251 (1994).

[2] L. A. Lugiato and F. Castelli, Phys. Rev. Lett. **68**, 3284 (1992).

[3] G. Grynberg and L. A. Lugiato, Opt. Commun. **101**, 69 (1993).

[4] L. A. Lugiato and G. Grynberg, Europhys. Lett. **29**, 675 (1995).

[5] A. Gatti and L. A. Lugiato, Phys. Rev. A **52**, 1675 (1995).

[6] M. I. Kolobov and I. V. Sokolov, Zh. Éksp. Teor. Fiz. **96**, 1945 (1989) [Sov. Phys. JETP **69**, 1097 (1989)]; Phys. Lett. A **140**, 101 (1989); Europhys. Lett. **15**, 271 (1991).

[7] A. La Porta and R. E. Slusher, Phys. Rev. A **44**, 2013 (1991).

[8] L. A. Lugiato and A. Gatti, Phys. Rev. Lett. **70**, 3868 (1993).

[9] M. I. Kolobov and L. A. Lugiato, Phys. Rev. A (to be published).

[10] V. Degiorgio and M. O. Scully, Phys. Rev. A **2**, 1170 (1970).

[11] R. Graham and H. Haken, Z. Phys. **237**, 31 (1970).

[12] G. L. Oppo, M. Brambilla, and L. A. Lugiato, Phys. Rev. A **49**, 2028 (1994).

[13] J. Mod. Opt. **34** (6/7) (1987), special issue on squeezed light, edited by R. Loudon and P. L. Knight, see in particular the introductory article by the editors.

[14] M. J. Collett and C. W. Gardiner, Phys. Rev. A **30**, 1386 (1984).

[15] D. F. Walls and G. J. Milburn, *Quantum Optics* (Springer-

Verlag, Berlin, 1994), pp. 127 and 128.
[16] See, e.g., *Handbook of Mathematical Functions*, edited by M. Abramowitz and I. Stegun (Dover, New York, 1965), pp. 771–788.
[17] A. Yariv, *Quantum Electronics*, 3rd ed. (Wiley, New York, 1989), pp. 136–154.
[18] M. J. Collett and D. F. Walls, Phys. Rev. A **32**, 2887 (1985); C. M. Savage and D. F. Walls, J. Opt. Soc. Am. B **4**, 1514 (1987).
[19] P. L. Knight *et al.* (unpublished).
[20] R. J. Glauber, Phys. Rev. **130**, 2529 (1963).
[21] M. I. Kolobov and P. Kumar, Opt. Lett. **18**, 849 (1993); P. Kumar and M. I. Kolobov, Opt. Commun. **104**, 374 (1994).
[22] L. A. Lugiato, G. L. Oppo, J. R. Tredicce, L. M. Narducci, and M. A. Pernigo, J. Opt. Soc. Am. B **7**, 1019 (1990).